Polyetheretherketone and titanium surface treatments to modify roughness and wettability – Improvement of bioactivity and antibacterial properties

Davide Porrelli*, Mario Mardirossian, Nicola Crapisi, Marco Urban, Nicola Andrea Ulian, Lorenzo Bevilacqua, Gianluca Turco, Michele Maglione

Department of Medical, Surgical and Health Sciences, University of Trieste, Piazza dell'Ospitale 1, 34129, Trieste, Italy

ARTICLE INFO

Article history:
Accepted 5 April 2021

Keywords:
PEEK
Titanium
Micropatterning
Roughness
Wettability
Differentiation

ABSTRACT

Among the materials available for implant production, titanium is the most used while polyetheretherketone (PEEK) is emerging thanks to its stability and to the mechanical properties similar to the ones of the bone tissue. Material surface properties like roughness and wettability play a paramount role in cell adhesion, cell proliferation, osteointegration and implant stability. Moreover, the bacterial adhesion to the biomaterial and the biofilm formation depend on surface smoothness and hydrophobicity. In this work, two different treatments, sandblasting and air plasma, were used to increase respectively roughness and wettability of two materials: titanium and PEEK. Their effects were analyzed with profilometry and contact angle measurements. The biological properties of the material surfaces were also investigated in terms of cell adhesion and proliferation of NIH-3T3 cells, MG63 cells and human Dental Pulp Stem Cells. Moreover, the ability of *Staphylococcus aureus* to adhere and form a viable biofilm on the samples was evaluated. The biological properties of both treatments and both materials were compared with samples of Synthegra® titanium, which underwent laser ablation to obtain a porous micropatterning, characterized by a smooth surface to discourage bacterial adhesion. All cell types used were able to adhere and proliferate on samples of the tested materials. Cell adhesion was higher on sandblasted PEEK samples for both MG63 and NIH-3T3 cell lines, on the contrary, the highest proliferation rate was observed on sandblasted titanium and was only slightly dependent on wettability; hDPSCs were able to proliferate similarly on sandblasted samples of both tested materials. The highest osteoblast differentiation was observed on laser micropatterned titanium samples, but similar effects, even if limited, were also observed on both sandblasted materials and air plasma treated titanium. The lowest bacterial adhesion and biofilm formation was observed on micropatterned titanium samples whereas, the highest biofilm formation was detected on sandblasted PEEK samples, and in particular on samples not treated with air-plasma, which displayed the highest hydrophobicity. The results of this work showed that all the tested materials were able to sustain osteoblast adhesion and promote cell proliferation; moreover, this work highlights the feasible PEEK treatments which allow to obtain surface properties similar to those of titanium. The results here reported, clearly show that cell behavior depends on a complex combination of surface properties like wettability and roughness and material nature, and while a rough surface is optimal for cell adhesion, a smooth and less hydrophilic surface is the best choice to limit bacterial adhesion and biofilm formation.

1. Introduction

The osteointegration is a fundamental process for implants and prostheses success, it consists in the formation of a strong and stable interface between the native tissue and the material, and it can be measured as the bone to implant contact. Material surface properties, as roughness and wettability, play a paramount role in the osteointegration process, since cell adhesion is the first event occurring between bone and the implant. Moreover, surface rough-

Abbreviations: hDPSCs, human Dental Pulp Stem Cells; P_M, machined PEEK samples; P_M*, machined and air-plasma treated PEEK samples; P_S, sandblasted PEEK samples; P_S*, sandblasted and air-plasma treated PEEK samples; Ti_L, laser micropatterned titanium samples; Ti_L*, laser micropatterned and air-plasma treated titanium samples; Ti_M*, machined and air-plasma treated titanium samples; Ti_S, sandblasted titanium samples; Ti_S*, sandblasted and air-plasma treated titanium samples.

* Corresponding author.
E-mail address: dporrelli@units.it (D. Porrelli).

ness is responsible for the mechanical retention of the implant within the bone defect [1,2].

Titanium and its alloys are the most used materials for the production of implant and prostheses; their chemical stability, mechanical properties and biocompatibility, make these metals the best choice for bone restoration procedures [3]. Despite its biocompatibility, titanium surface needs to be modified in order to improve cell adhesion, cell proliferation and osteointegration [3–6]. The most exploited strategy is the increase of surface roughness by means of additive (plasma spray, ion deposition, surface coating) or subtractive (sandblasting, chemical etching) techniques [7,8]. Roughness increase is related with an enhancement of surface wettability, which improves cell adhesion [9]. Unfortunately, these surface features promote also bacterial adhesion [10,11].

Implant and prostheses colonization by bacteria is a critical issue in the clinical practice; this phenomenon can lead to implant failure and tissue damage, and can require additional surgery for the removal of the contaminated material [12]. Several strategies, as silver ion or silver nanoparticles implantation, antimicrobial peptides coatings, polycations and antibacterial polysaccharides coatings to name some, have been investigated to provide antibacterial properties to titanium surfaces [13–15]. A novel treatment of laser ablation (Synthegra®, Geass s.r.l., Italy) represents an interesting strategy which can promote cell adhesion, and at the same time limit bacterial adhesion to the material surface. This treatment is used to obtain micropatterned pores on a smooth titanium surface and demonstrated to improve on one side eukaryotic cell adhesion, and, on the other, inhibit bacterial adhesion [2,16,17].

Despite the excellent results achieved over the years with the use of titanium implant and prostheses, there is an effort for the research of novel materials for the replacement of titanium, whose use is limited by the manufacturing process, lack of bioactivity, delayed healing, stress shielding risk and high production costs [18,19]. Among the materials studied for titanium replacement, polyetheretherketone (PEEK) is emerging as a valid alternative [19,20]. The chemical structure of this polymer is responsible for its excellent thermal stability and resistance to chemical and radiation damages [21]. Therefore, after the sterilization processes obtained by irradiation or chemical treatments, PEEK resulted to maintain its features and this represents an advantage if compared with other polymeric materials [22,23].

PEEK mechanical properties (*i.e.* mainly elastic modulus), are similar to those of the native bone tissue, reducing therefore the risk of stress shielding and implant failure and making this material very promising in both dental and orthopedic fields [18]. With respect to titanium, the manufacturing process of PEEK is also advantageous; PEEK can be associated to CAD-CAM techniques and used for 3D printing and rapid prototyping, exploiting fused deposition model techniques [24–26]. Moreover, PEEK can be enriched with carbon or glass nanofibers, and used for the preparation of nanocomposites with tailored mechanical properties [27–29]. The use of PEEK as a biomaterial for orthopedic prostheses and implants started at the end of the '80s [30], and from the end of the '90s has been proposed as a possible substitute to metallic implants [31] with the first commercialization of a PEEK based implants dated in 1998 [32]. Since then, PEEK has been extensively used in orthopedic and spine surgery [30]. Only recently, PEEK has started to be considered for the preparation of dental implants and abutments but further clinical trials are necessary to investigate PEEK use as a dental material [31]. Several *in vitro* studies proved PEEK biocompatibility and *in vivo* studies demonstrated the successful use of PEEK for production of fixation rods and plates, spinal fusion cages, implants, abutments and prostheses with performances similar to titanium ones [18,33–37].

The main drawback of PEEK is its biological inertness, which hampers cell adhesion and implant osteointegration [38]; thus, likewise to titanium, its surface has to be treated to improve its biological properties [39]. Surface modification of PEEK is achieved with additive and subtractive strategies, as for example, sandblasting, hydroxyapatite implantation, plasma spray, acid etching and micropatterning, in order to tailor roughness, wettability and bioactivity [31,39,40]. Moreover, PEEK surface can be functionalized in order to introduce antibiotics and antimicrobial compounds like silver nanoparticle and polycations [41–44].

Among the techniques available to improve surface wettability, air-plasma cleaning process is a cost-effective technique widely applied in industrial processes [40,45], which can be used to modify materials based on PEEK, polytetrafluoroethylene (PTFE) and polydimethylsiloxane (PDMS) [46,47] and can be also applied to titanium [48]. This process introduces polar groups, such as carboxylic groups, on the material surfaces and, consequently, increases the polar component of the surface energy therefore improving surface wettability [47–49].

In this work, the effects of sandblasting and air-plasma treatments on surface roughness and wettability were evaluated for both titanium and PEEK samples. The surfaces were compared with Synthegra® titanium, which were also subjected to air-plasma treatment. The biological properties were assessed in terms of cell adhesion proliferation and osteoblast differentiation using fibroblasts, osteoblasts and human Dental Pulp Stem Cells (hDPSCs) to take account of the tissues involved in prostheses and implant osteointegration and fibrointegration. hDPSCs are a pluripotent population of stem cells with genetic stability, able to generate calcified colonies and to differentiate into osteoblasts, chondrocytes, cardiomyocytes, neuron, liver cells and β cells of islet of pancreas [50]. Their use was suggested for tissue engineering applications [51] and as a cell model for the evaluation of biomaterials biological properties for dental materials [52,53]. Moreover, *Staphylococcus aureus* was used to test the bacterial adhesion and biofilm formation on sample surfaces. This pathogen is frequently isolated in the oral cavity [54], it efficiently adheres on titanium surfaces and has been associated with the early failure of titanium based dental implants [55,56].

2. Materials and methods

2.1. Materials

Disks with a diameter of 8 mm and a height of 4 mm of machined titanium, laser treated titanium (Synthegra treatment) and machined PEEK were used. Titanium samples were provided by Geass S.r.l. (Udine, Italy), PEEK samples were purchased from Robecchi S.r.l. (Bergamo, Italy). Sandblasting treatment was performed using aluminum oxide powder (125 μm) at 3 atm of pressure. Several conditions were tested varying the distance and the exposure time, in order to achieve similar roughness between titanium and PEEK, with values comparable with the literature [1,25,57]. The optimal protocol involved the treatment of PEEK for 10 s at 5 cm of distance, and the treatment of titanium for 20 s at 2 cm of distance. Sandblasted samples were washed in deionized water for 30 s and with an aqueous vapor jet, then dried with compressed air. Air plasma treatment was performed using a PDC-32G Plasma Cleaner (Harrick Plasma, Ithaca, New York, USA) at 6.8 W (8–12 MHz of frequency) for 5 min. Dulbecco's Modified Eagle Medium (DMEM), Fetal Bovine Serum (FBS), penicillin/streptomycin, L-glutamine, trypsin, were purchased from Euroclone (Italy). Collagenase I, dispase, ascorbic acid, Phosphate Buffered Saline (PBS), Luria Bertani's culture medium (LB), Sodium Dodecyl Sulfate (SDS), MTT (3- [4,5- dimethylthiazol-2-yl]-2,5-diphenyl tetrazolium bromide) were purchased from Sigma Aldrich (USA). All the other chemicals were of analytical grade and were purchased from Sigma Aldrich (USA). Complete DMEM was pre-

pared adding heat inactivated FBS 10%, penicillin 100 U/mL, streptomycin 0.1 mg/mL, L-glutamine 2 mM.

2.2. Surface roughness

Surface roughness analysis was performed using a profilometer Talysurf CLI 1000 (Taylor Hobson, Berwyn, Pennsylvania, USA), acquiring for each sample, 5 linear profiles with 4 mm length. 7 samples were analyzed for each material and each treatment.

2.3. Surface wettability

Surface wettability was analyzed measuring the contact angle, using the "*sessile drop technique*", measuring the angle formed by a drop of deionized water with the material surface. For each material 7 samples were analyzed, measuring the contact angle of 2 drops of 4 μL of deionized water. Images were acquired with a Leica MZ16 stereo microscope, equipped with a Leica DFC 320 digital camera (Leica Biosystems Nussloch, Germany). Images were acquired 30 s after drop deposition in order to have a stable drop, and were analyzed with Image ProPlus software (MedyaCibernetics, USA).

3.3. Microhardness evaluation

Microhardness of samples before and after sandblasting and airplasma treatments was measured using a Leica VMHT MOT (Walter Uhl, Asslar, Germany) hardness tester equipped with a Vickers indenter applying a load of 100 g for 10 s. Five measurements were taken and averaged for each sample.

2.5. Morphological analyses and microanalyses

Morphological analyses and microanalyses were performed with a Scanning Electron Microscope Quanta250 (FEI, Oregon, USA.), in high vacuum, in secondary electron mode, with 30 kV of tension and 10 mm of working distance. Samples were mounted on aluminum stubs with a carbon double-sided tape. For the morphological analyses PEEK samples were gold sputtered with a Sputter Coater K550X (Emitech, Quorum Technologies Ltd, UK); for the microanalysis, PEEK samples were coated with a carbon layer using the Sputter Coater K550X coupled with the CA7625 Carbon Accessory (Emitech, Quorum Technologies Ltd, UK). Microanalysis was performed by Energy Dispersive Spectroscopy using an Apollo X EDAX probe (EDAX, Mawah, New Jersey, USA) coupled with the SEM; X-ray spectra were collected for 120 s.

2.6. Cell cultures

Osteosarcoma derived human osteoblasts MG63 (ATCC® CRL-1427™) and murine fibroblast (ATCC® CRL-1658™) were cultured in complete DMEM in humid atmosphere at 37 °C with 5% pCO_2. Cell were passed using trypsin twice a week when confluency reached 80–90%. Human Dental Pulp Stem Cells (hDPSCs) where extracted from third molars removed for surgical reasons, with the informed consent from the patient (Authorization by Regional Health Service- Azienda Sanitaria Universitaria Integrata di Trieste and by the Comitato Etico Unico Regionale - CEUR FVG, ID studio 2433: TERM – "Collection of biological samples for the study of biocompatibility and bioactivity on dental pulp cells of materials for restorative and regenerative dentistry"). The extracted teeth were immediately soaked in sterile PBS with antibiotics (penicillin 500 U/mL and streptomycin 500 mg/mL). A microtome (IsoMet™ Low Speed Saw, BUEHLER, China) was used to expose the pulp chamber, which was finely cut and incubated for 45 min, in humid atmosphere at 37 °C with 5% pCO_2, in a 5 mL of a mix composed by PBS, 500 U/mL penicillin, 500 mg/mL streptomycin, 2.4 mg/mL collagenase I and 3.2 mg/mL dispase. Protein digestion was then stopped with 3 mL of complete DMEM and the digested dental pulp was centrifuged at 800 rpm for 5 min. The resulting pellet was suspended with complete DMEM added with ascorbic acid 100 μM. Cells were cultured in complete DMEM in humid atmosphere at 37 °C with 5% pCO_2. Cell were passed using trypsin twice a week when confluency reached 70%-80%.

2.7. Analysis of cell adhesion and proliferation

For each material and treatment, 6 samples were used for cell adhesion and proliferation, and 2 as blanks. Samples were UV sterilized and placed in a 48 multi-well plate not treated for cell adhesion (Sarstedt, Numbrecht, Germany). MG63 and NIH-3T3 were cultured in complete DMEM, hDPSCs were cultured in complete DMEM added with ascorbic acid 100 μM. On each sample, 3000 cells suspended in 50 μL of culture medium were seeded; after 4 h of incubation in humid atmosphere at 37 °C with 5% pCO_2, 200 μL of culture medium were added. Cell adhesion and proliferation were evaluated thanks to Resazurin Cell Viability Assay Kit (Biotium, Fremont, CA, USA), tests were performed at 1, 3, 6 and 9 days. For each experimental time point, culture medium was removed and for each sample, 200 μL of DMEM with 10% of resazurin solution were added. After 4 h of incubation, 150 μL were withdrawn for fluorescence measurement; each well was washed with PBS and 200 μL of culture medium were added. Fluorescence measurements were performed with a GloMax Multi+ Detection System spectrofluorometer (Promega, USA) with an excitation wavelength of 525 nm and collecting the emitted fluorescence in the range 580–640 nm. For each condition, at day 1 and day 9, two additional samples were prepared as described above, for the evaluation of adhesion and proliferation with SEM imaging.

2.8. Alkaline phosphatase activity

For each condition and time point, 5 samples were used for cell adhesion, and 2 as blanks. Samples were UV sterilized and placed in a 48 multi-well plate not treated for cell adhesion (Sarstedt, Numbrecht, Germany). hDPSCs were cultured in complete DMEM added with ascorbic acid 100 μM. On each sample, 10000 cells suspended in 40 μL of culture medium were seeded; after 4 h of incubation in humid atmosphere at 37 °C with 5% pCO_2, 200 μL of culture medium were added. Alkaline phosphatase activity was evaluated at day 4, day 7 and day 14. For each experimental time point, culture medium was removed and samples were washed with PBS. After PBS removal, cells were lysed in 400 μL of lysis buffer (Tris-HCl 100 mM; Triton X100 2% v/v) at -20 °C for 30 min. Samples were collected in micro tubes and centrifuged at 13000 round per minute (rpm) for 10 min. ALP enzymatic activity was measured in a solution of 6 mM para-nitro-phenyl-phosphate and 1 mM $MgCl_2$ in Tris-HCl, 100 mM, pH 9.8, after 60 min of incubation at 37 °C. Absorbance was measured at 420 nm with the FLUOstar® Omega plate reader (BMG Labtech, Ortenberg, Germany). The results were normalized to the amount of protein content in the cellular extract calculated by means of the Pierce Micro BCA Protein Assay Kit (Thermofisher, Waltham, MA, USA) according to manufacturer's protocol. For each condition and time point, two additional samples were prepared as described above, for the evaluation of adhesion and proliferation with SEM imaging.

2.9. Biofilm formation

Biofilm formation on material surfaces was tested on *Staphylococcus aureus* ATCC 25923 using the MTT test to assess biofilm viability. For each material and each treatment, 14 samples were an-

alyzed (two of which used as blanks); samples were UV-sterilized and placed in sterile 6-well plates. Bacteria were grown on an LB agar plate at 37 °C and subsequently few colonies were inoculated overnight in 4 mL of LB liquid medium at 37 °C under agitation (140 rpm). The following day a re-inoculum was performed diluting 200 μL of the overnight culture in 10 mL of new LB medium. The new culture was grown for about 1 h and 30 min, in agitation (120 rpm), at 37 °C until reaching an optical density (OD) equal to about 0.3 measured at 600 nm. The concentration of bacteria in re-inoculate was then calculated considering the empirical observation that OD600 = 0.1 for this strain corresponds to 5×10^7 bacteria/ml and making a simple proportion. Bacteria were then diluted to a final concentration of 10^6 CFU/ml in new LB medium. 50 μL of bacterial suspension were placed on the surface of each sample; sterile deionized water was added between the wells in order to prevent medium evaporation, and the multiwell plates were incubated overnight at 37 °C in a humid atmosphere. The day after, samples were washed with PBS in order to remove not adhered bacteria, and each sample was transferred in a 48 well plate with 300 μL of MTT 1 mM diluted in LB medium. The multiwell plate was incubated in the dark, at 37 °C for 4 h. After the incubation, the medium was removed and samples were washed with 400 µL of PBS. MTT crystals were solubilized with 300 μL of lysis solution (20% SDS in deionized water/dimethylformamide 1:1). The multiwell plate was incubated overnight at 37 °C in dark conditions. After the incubation, 100 μL were taken from each well and deposited in a 96-well microtiter plate; the absorbance at 570 nm was read using a Nanoquanta infinite M200pro spectrophotometer (Tecan, Switzerland) and the biofilm viability was calculated as a function of the OD570. For each condition and time point, two additional samples were prepared as described above, for the evaluation of adhesion and proliferation with SEM imaging.

2.10. SEM observation of cells and bacteria

Samples were washed with PBS and fixed with formaldehyde (4% in PBS) for 45 min at each experimental time point. Samples were then washed with deionized water and dehydrated by stepwise treatment with ethanol in water (30%, 50%, 70%, 90%, 100%), and then with hexamethyldisilazane in ethanol (30%, 50%, 70%, 90%, 100%). After 1 h in hexamethyldisilazane 100% samples were air-dried, sputter-coated with gold and visualized by scanning electron microscopy as previously described.

2.11. Statistical analysis

Statistical analysis was performed with OriginPro software (OriginLab Corporation, Northampton, Massachusetts, USA). Biofilm viability, roughness, wettability, microhardness and EDS data did not satisfied normality (Kolmogorov-Smirnov's test) and homoscedasticity (Levene's test) and were analyzed by Kruskal-Wallis test and a Mann-Whitney U test for pairwise comparisons, applying a Bonferroni correction. Cell adhesion and proliferation data satisfied normality and homoscedasticity conditions and were analyzed with an ANOVA test applying Tukey's post-hoc correction. Statistical significance was pre-set at $\alpha = 0.05$.

3. Results

In all the analyses reported, samples are indicated as follow: Ti_M, machined titanium; Ti_S, sandblasted titanium; Ti_L, laser treated titanium; P_M, machined PEEK; P_S, sandblasted PEEK. Samples subjected to air-plasma treatment are indicated with an asterisk (*).

3.1. Surface roughness analysis

Profilometry was used to investigate the effects of the sandblasting and the air-plasma treatments. The investigation was performed preliminarily to set the optimal parameters of sandblasting process, to obtain similar roughness between Ti_S e and P_S samples (data not showed). The native roughness of samples and the effects of the treatments applied are reported in Fig. 1. From the results, the difference between the native samples of P_M and Ti_M can be noticed; moreover, after sandblasting the roughness of Ti_S and P_S was higher with respect to the native samples. Ti_S and P_S after the treatment reached comparable roughness, even if a statistically significant difference was still verified ($p < 0.05$).

Then the impact of the air-plasma treatment on the sample morphology was evaluated. The procedure did not have an effect on the roughness with the exception of Ti_L samples, which displayed a slight, even significant, decrease of roughness in Ti_L* samples. SEM micrographs, reported in Fig. SI-1 allow to appreciate the differences in the surface morphology between Ti_L (Fig. SI-1A) and Ti_L* (Fig. SI-1B) samples, the latter appearing smoother than the former, probably because of a cleaning effect of the air-plasma treatment.

Profilometry was also used for the analysis of surface morphology in terms of skewness (reported in Fig. SI-2A) and kurtosis (reported in Fig. SI-2B). Data show the differences of the untreated samples of Ti_M, P_M and Ti_L and in particular, the negative value of skewness for Ti_L samples, which indicates the presence of pores. Moreover, in all cases, the air-plasma treatment did not have an effect on these values ($p > 0.05$). The sandblasting process, both for titanium and PEEK, led to a relevant and statistically significant ($p < 0.05$) variation of skewness and kurtosis, indeed after sandblasting the surfaces displayed a more symmetric (skewness closer to 0) and a more Gaussian-like (kurtosis closer to 3) roughness profile. Skewness and kurtosis were similar between sandblasted titanium and PEEK samples ($p > 0.05$).

3.2. Surface wettability analysis

Surface hydrophilicity was evaluated measuring the wettability of the sample with the contact angle technique, using the sessile drop approach. Contact angle values are reported in Fig. 2. The lowest wettability among samples not subjected to air-plasma treatment, was observed for P_S and Ti_L samples. After the air-plasma treatment, a statistically significant increase of wettability was observed for all samples with the exception of machined PEEK samples.

3.3. Microhardness evaluation

In order to furhter investigate the effects of the sandblasting and air-plasma treatments on samples, microhardness was measured before and after both treatments. Representative images of indentation on samples surfaces are reported in Fig. SI-3A-J and the quantitative results are reported in Fig. SI-4. The analysis of the results demonstrated that both sandblasting process and air-plasma cleaning process did not significantly ($p > 0.05$) alter the microhardness of samples.

3.4. Morphological investigation and microanalysis

The qualitative analysis of sample morphology after sandblasting and air-plasma treatment was performed with SEM. The images reported in Fig. 3 clearly show the differences between the smooth surfaces of machined samples, the rough surface of sandblasted samples and the micro-patterned surface of laser treated ones. At a macroscopic level, there were no differences between

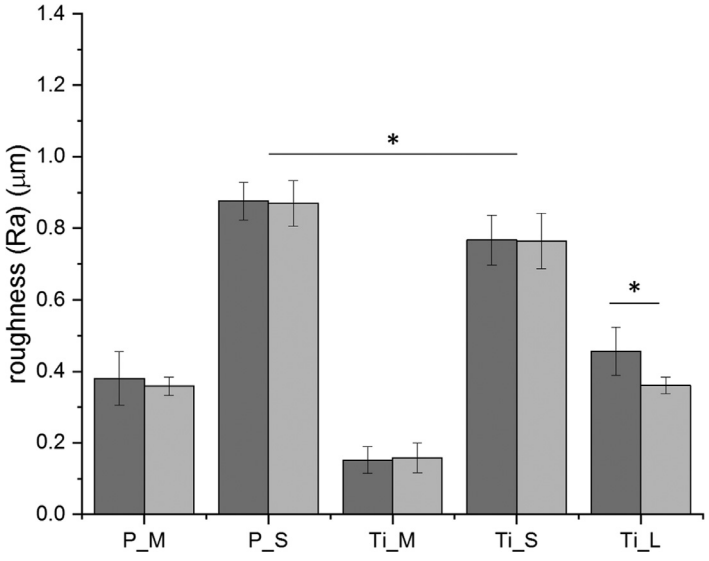

Fig. 1. Effects of treatments on surface roughness. Roughness values of titanium and PEEK samples before (grey) and after (light grey) air-plasma treatment. Relevant comparisons are indicated with an asterisk ($p < 0.05$) or with NS (not significant).

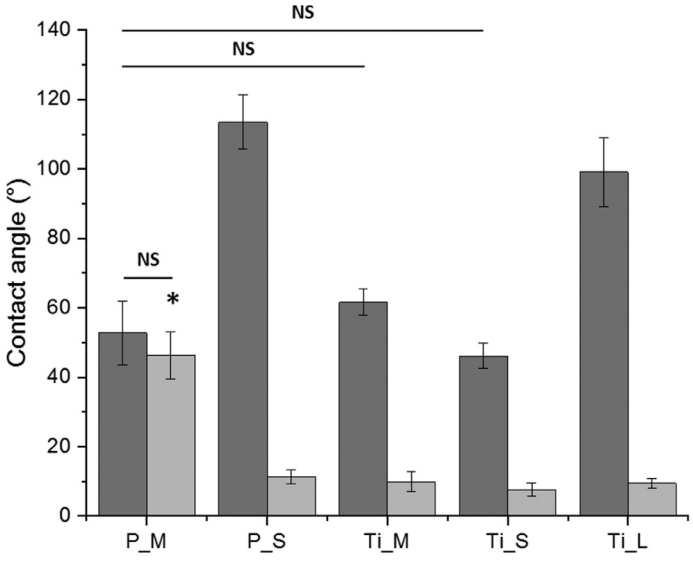

Fig. 2. Effects of treatments on wettability. Wettability, expressed with the contact angle, of sample surfaces before (dark grey) and after (light grey) air-plasma treatment. Relevant comparisons are indicated with an asterisk ($p < 0.05$) or with NS (not significant).

native and air-plasma treated samples, with the exception of laser treated titanium ones, as observed in Fig. 2.

In Fig. 4, the morphology of PEEK samples is reported. As observed for the ones belonging to the titanium group, the differences between the smooth surfaces of machined samples and the rough surface of sandblasted ones can be appreciated.

Energy Dispersive Spectroscopy was performed in order to investigate the presence of contaminants on sample surface and to quantify the presence of alumina residues after the sandblasting process. The energy spectra are reported in Fig. SI-5A-F and the quantification of aluminum in reported in Fig. SI-6. The quantification of aluminum revealed differences in the effects of sandblasting process between PEEK and titanium, as on PEEK surfaces the amount of aluminum was one order of magnitude lower with respect to titanium surface. Moreover, a slight and statistically significant decrease of aluminum content was observed for sandblasted PEEK samples after air-plasma treatment.

3.5. Cell adhesion

The ability of cells to adhere on titanium and PEEK substrates was correlated to surface morphology and wettability, using three different cell types: murine fibroblasts (NIH-3T3), human osteoblasts (MG63) and human Dental Pulp Stem Cells (hDPSCs). Cell adhesion was measured as the intensity of the Alamar Blue fluorescence signal after 1 day of cell culture. The highest NIH-3T3 cell adhesion (Fig. 5(A)) was detected on P_S and P_S* samples with no statistically significant difference between the values for these two groups. MG63 cell adhesion (Fig. 5(B)) is similar among samples with the exception of P_S*, for which a higher cell adhesion was observed. Regarding hDPSCs adhesion (Fig. 5(C)) no statistically significant differences were detected among materials tested.

SEM micrographs, reported in Fig. SI-7, collected after 1 day of cell culture allowed the qualitative evaluation of cell morphology. In all cases, cells showed healthy morphology and spread on the whole sample surfaces, with the cellular adhesion processes correctly in contact with the surface.

3.6. Cell proliferation

Cell proliferation on the different samples was evaluated over time, up to 9 days of cell culture, normalizing the values of Alamar Blue fluorescence intensity at 3, 6 and 9 days with the values of day 1 for NIH-3T3 cells (Fig. 6(A)), for MG63 cells (Fig. 6(B)) and for hDPSCs (Fig. 6(C)). Both for MG63 cells and for hDPSCs, the increase of proliferation rate over time was statistically significant ($p < 0.05$). For NIH-3T3 cells, in all cases, the proliferation rate at day 9 was similar to day 6 ($p > 0.05$), indicating that cell confluence might be reached.

Regarding NIH-3T3 cells, sandblasted titanium was the best performing material, with respect to sandblasted PEEK or laser-treated titanium. Air-plasma treatment did not affect the proliferation ability of cells with the exception of laser-treated titanium (Ti_L*), which showed the worst performances.

The MG63 cells showed the best proliferation rate when cultured on sandblasted titanium samples in particular on TI_S*; whereas, Ti_L* was the material with the lowest proliferation rate.

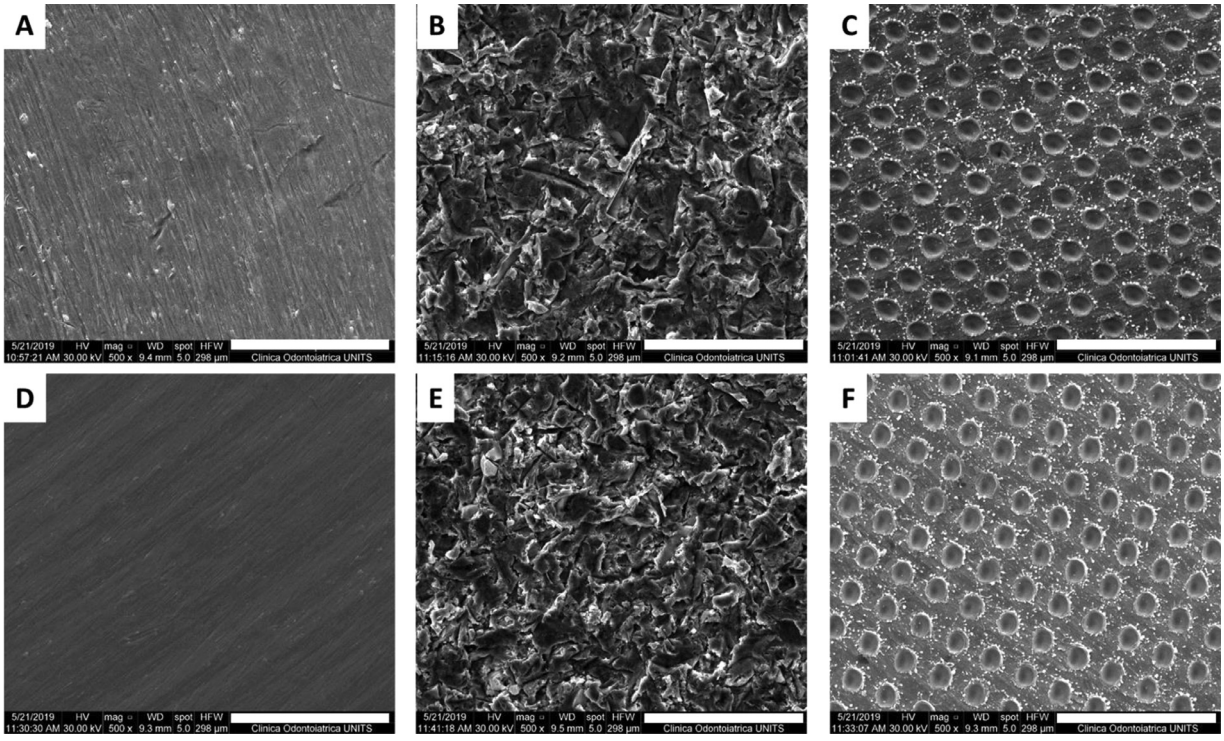

Fig. 3. Titanium surface morphology. SEM micrographs of titanium samples surfaces: Ti_M (A), Ti_M* (D), Ti_S (B), Ti_S* (E), Ti_L (C), Ti_L* (F). Scale bar is 100 µm.

PEEK samples showed an intermediate behavior without any statistically significant difference when treated with air-plasma process.

The hDPSCs showed a similar behavior on sandblasted titanium and sandblasted PEEK samples, without differences between not treated or air-plasma treated samples. From 6 to 9 days of proliferation, cells displayed a slowdown of metabolic activity on laser-treated titanium samples.

SEM micrographs collected after 9 days of cell culture are reported in Fig. SI-8. In all cases, it is possible to appreciate the almost complete coverage of sample surfaces with a uniform cell layer, in which cells were not distinguishable. On all the materials tested, cells were able to adhere and proliferate, to spread on the surface and to deposit extracellular matrix.

3.7. Alkaline phosphatase activity

In order to better understand the behavior of hDPSCs when cultured on the tested substrates, the differentiation towards an osteoblast phenotype was assessed measuring the alkaline phosphatase (ALP) activity. The results reported in Fig. 7 show that, over time, hDPSCs start to express ALP and to differentiate on all the substrates tested, with differences related to the material nature and the surface modification. A statistically significant increase of ALP activity over time can be appreciated for cells cultured on P_S, Ti_S*, Ti_L and Ti_L* samples. An increase of ALP activity can be appreciated also for hDPSCs seeded on P_S* and Ti_S samples, although the ALP activity at day 7 and day 14 is not significantly higher than the ALP activity at day 4. Regarding the differences among materials, noteworthy, the ALP activity of hDPSCs cultured on Ti_L and Ti_L* samples, is significantly higher than the ALP activity of cells cultured on Ti_S, Ti_S* and P_S* samples. It is also interesting to point out the statistically significant positive effect of the air-plasma treatment on ALP activity only for Ti_S* samples (if compared with Ti_S samples).

SEM micrographs of hDPSCs cultured on the tested materials for the ALP activity assay, collected at the tested time points, are reported in Fig. SI-9, SI-10 and SI-11 at different magnifications. In all cases, it is possible to appreciate the wide spread adhesion of hDPSCs on all the materials, and the colonization of the surface over time. The images collected after 14 days of cell culture confirm that there are not differences, among the materials and the surface treatments, in terms of hDPSCs proliferation and materials surface colonization. These data, together with the ALP activity, demonstrate that the slowdown of metabolic activity reported in Fig. 6(C) may be due to the changes in the cell phenotype and is not a slowdown of cell proliferation.

3.8. Biofilm formation and growth

The ability of *Staphylococcus aureus* to adhere and grow on the materials tested, and to form a viable biofilm, was tested with a MTT assay (Fig. 8). The highest formation of biofilm was observed on P_S samples, followed by P_S* samples. Titanium surfaces are less prone to the biofilm formation and behave in a similar way, with the exception of Ti_L samples, which show the lowest presence of biofilm.

A qualitative evaluation of the bacterial adhesion can be provided by SEM analysis reported in Fig. 9. From the images it can be appreciated the lowest bacterial adhesion and growth on Ti_L samples (Fig. 9(C)) and the highest bacterial adhesion and growth on PEEK samples, in particular on hydrophobic ones (Fig. 9(A)) not activated with air-plasma treatment.

4. Discussion

Surface modification approaches are fundamental strategies for the implementation of osteointegration and other biological properties of implants and prostheses [4,31,38,39]. This study compared the effects of roughness and wettability modifications on the interactions with bacteria and eukaryotic cells of two biomaterials: PEEK and titanium. A micro-patterned titanium surface developed by Geass S.r.l. [16,17], which possesses low hydrophilicity [57], was

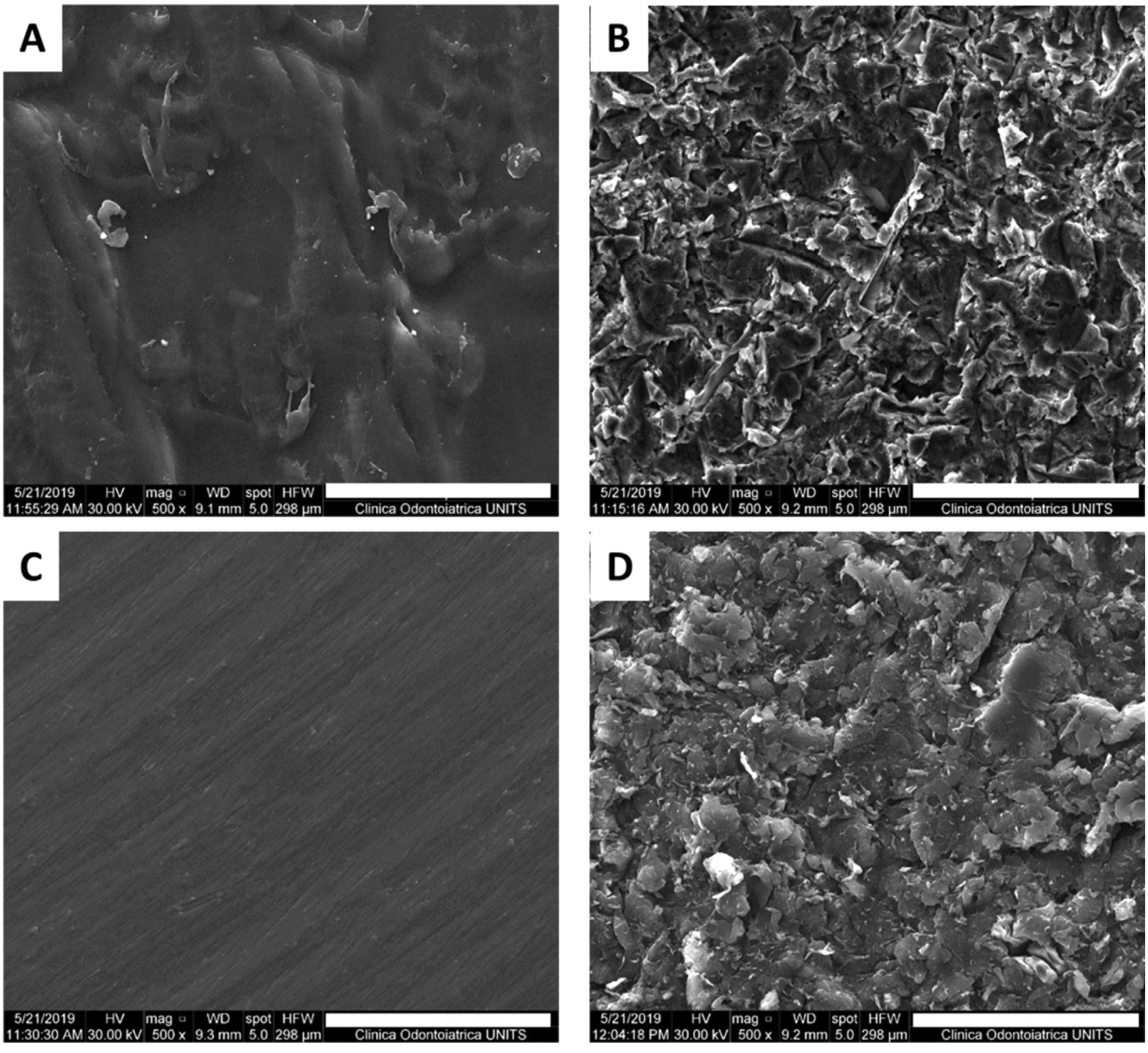

Fig. 4. PEEK surface morphology. SEM micrographs of PEEK samples surfaces: P_M (A), P_M* (C), P_S (B), P_S* (D). Scale bar is 100 µm.

used for comparisons, and was also subjected to the same treatment (*i.e.* air-plasma) of the tested groups for improve wettability. On the tested samples, sandblasting with alumina powder and air-plasma treatment, were used to improve respectively roughness and wettability. These techniques have been widely used for the surface modification of titanium implants and prostheses, and for the modification of polymeric biomaterials like PEEK, PTFE and PDMS [39,40,46,58]. These two surface modification techniques are commonly applied in industrial processes, are cost effective and do not require complex protocols or the use of toxic or hazardous compounds [3,45,59,60]. Process parameters of sandblasting and air-plasma treatment were chosen and tuned to obtain similar roughness and wettability between titanium and PEEK, in order to standardize the morphology and chemistry of surfaces tested. Profilometry measurements showed that the treatments applied led to an increase of surface roughness for both titanium and PEEK samples, and that the roughness and morphology obtained were comparable between the materials and the studies reported in literature for an optimal osteointegration [24,57,61]. Air-plasma treatment led to an increase of surface hydrophilicity for all the surfaces tested with the exception of machined PEEK samples; it can be hypothesized that the morphological alteration, *i.e.* the increase of active surface, caused by sandblasting makes PEEK more susceptible to the air-plasma treatment with respect to the unaltered PEEK surface [20,62,63]. Wettability data obtained on sandblasted and air-plasma treated PEEK surfaces are not directly comparable with the literature, as different results have been obtained depending on the specific treatment: El Alwadly *et al.* observed an increase of PEEK wettability after sandblasting, with a roughness between 1 and 15 µm [1]; Han *et al.* showed a decrease of wettability for roughness values below 1 or above 1.7 µm [24]; and more interestingly, Akkan *et al.* observed an increase of PEEK hydrophobicity when treated with a laser micropatterning technique combined with an oxygen plasma treatment [40]. In this case, contact angle measurements confirmed the hydrophobicity of sandblasted PEEK reported in literature [64,65], due to the fact that an increase of the surface roughness increases its hydrophobic behavior [66] and the increase of wettability subsequent to the air-plasma treatment [67,68]. Surface microhardness evaluation on all the materials tested, before and after sandblasting or air plasma treatment processes, showed that this property is not affected by the surface treatments here applied, and that the microhardness values are similar to those reported in literature [69,70]. A critical issue resulted from the EDS analysis of sandblasted samples, is the presence of alumina residues, which presence is much lower on PEEK samples with respect to titanium samples. Despite the

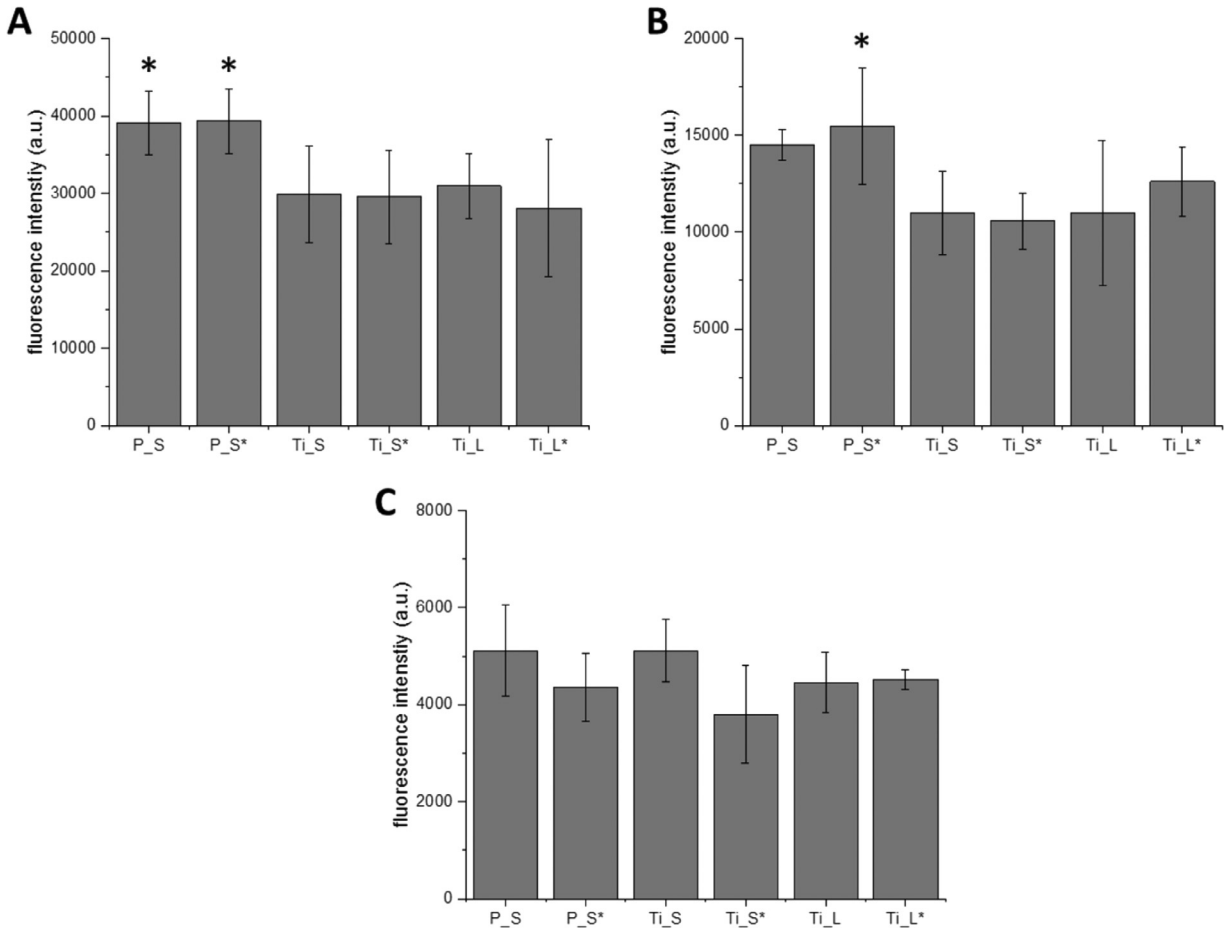

Fig. 5. Cell adhesion on treated samples. Cell adhesion measured for NIH-3T3 cells (A), MG63 cells (B) e hDPSCs (C) and expressed as the fluorescence intensity of the Alamar Blue. The asterisks indicate relevant statistically significant differences between samples for the same cell line ($p < 0.05$).

proven biocompatibility of alumina [71,72] and the lack of any adverse effect on osseointegration of alumina residues [73], it has been suggested that alumina presence might exert long-term negative effects on osseointegration [74]. In this context some strategies have been proposed to remove alumina residues, such as the acid etching of SLA titanium surfaces [75], or to stabilize the surface in order to avoid the release of aluminum ions with a thermal treatment [76]. Future studies, to be performed comparing the surfaces here tested, with titanium SLA surfaces [75] and acid etched PEEK surfaces will be necessary to determine the effect of the alumina residues here observed.

The biological properties of the materials, depending on the surface morphology and chemistry, have been evaluated using murine fibroblasts (NIH-3T3) and human osteoblasts (MG63), in order to consider the involvement of bone and gingival tissue in the implant integration [77–79]. Moreover, human Dental Pulp Stem Cells (hDPSCs) were used to test the ability of the materials here analyzed, to sustain cell differentiation [6]; to the best of the authors' knowledge, this is the first time that the osteogenic properties of PEEK and titanium, subjected to the surface treatments here tested, are evaluated using hDPSCs and compared. Cell adhesion and the proliferation have been both evaluated using the fluorescence signal of the Alamar Blue assay: indeed, the correlation between its fluorescence intensity and the cell number is well documented [80,81], moreover the Alamar Blue has been recently used for the evaluation of cell adhesion on biomaterials [82].

NIH-3T3 showed a preferential adhesion on PEEK surfaces independently from the wettability, but the best performances in terms of proliferation were observed when fibroblasts were cultured on sandblasted titanium surfaces. In the literature, a similar behavior between PEEK and titanium is reported in terms of fibroblast and keratinocyte adhesion and proliferation [83,84], but a preferential adhesion has been reported for micro-machined titanium surfaces with respect to polished ones [85]. The air-plasma treatment effects were observed only for laser-treated titanium samples, which were less prone to favour cell proliferation when subjected to the treatment; it has been reported that surface hydrophilicity can impair fibroblast adhesion, spreading and protein expression [86].

Osteoblasts cells were able to adhere on all the surfaces without any statistically significant difference, with the exception of MG63 cells, which showed the best adhesion on sandblasted and air-plasma treated PEEK surfaces. Regarding the proliferation, the highest proliferation rates were observed on sandblasted titanium samples, followed by sandblasted PEEK and by laser micropatterned titanium samples. In the literature, the positive effects on osteoblast proliferation of sandblasting and surface activation of titanium have been reported [87]. The literature about osteoblast behavior on PEEK and titanium is controversial; depending on the surface topography and hydrophilicity different behaviors have been documented. Benz *et al.* reported a similar behavior of osteoblasts seeded onto machined PEEK samples, presenting a grinding pattern, and rough titanium samples [83]. da Cruz *et al.* cultivated osteoblasts on sandblasted and acid etched PEEK and titanium samples, observing a higher proliferation on PEEK samples [78], but Najeeb *et al.* observed a higher osteoblast proliferation and maturation on titanium samples with respect to PEEK samples [38]. The results presented in this work show that all the materi-

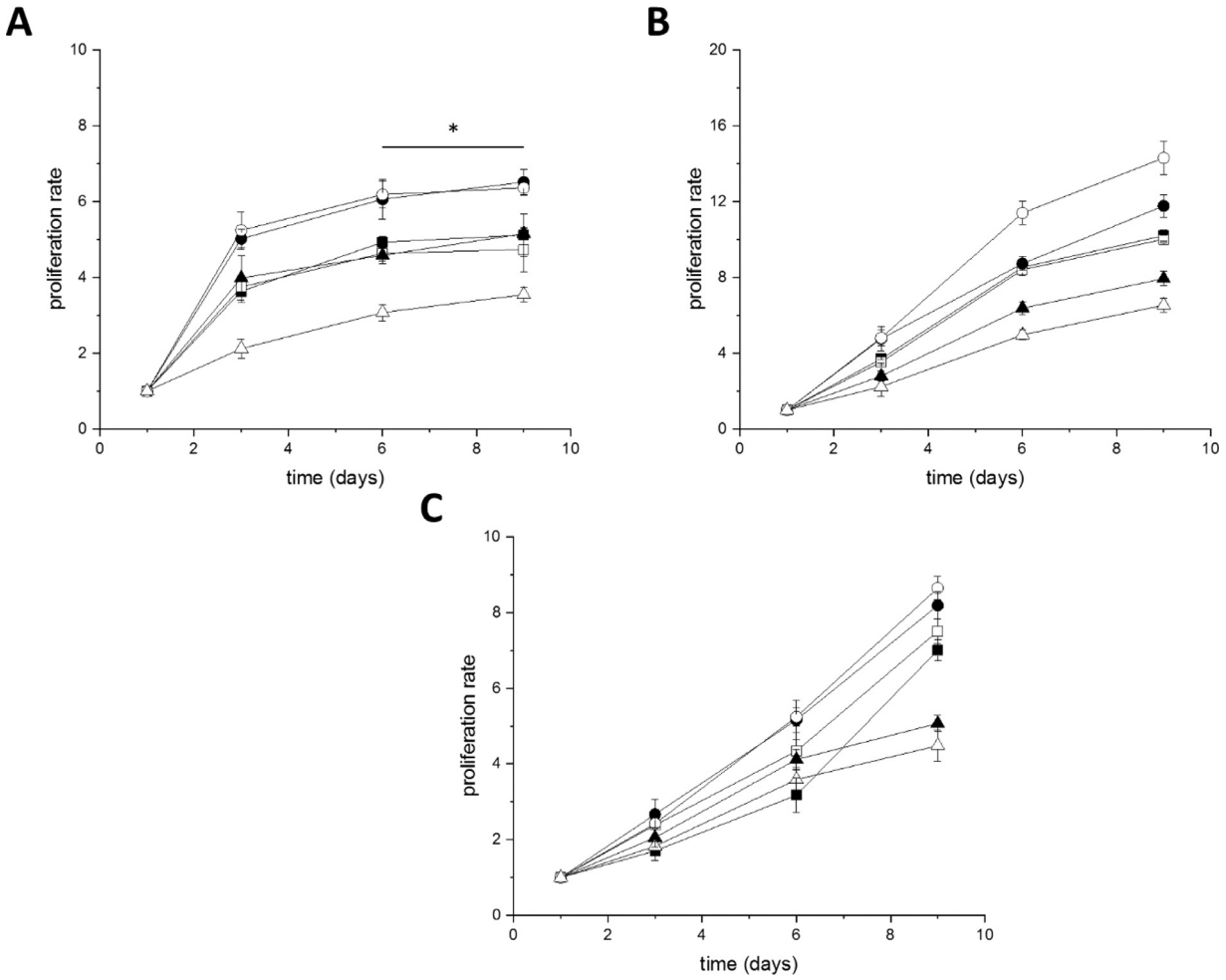

Fig. 6. Cell proliferation on treated samples. Proliferation rate trends for NIH3T3 cells (A), MG63 cells (B) and hDPSCs (C) cultured on titanium and PEEK samples. (■, P_S; □, P_S*; ●, Ti_S; ○, Ti_S*; ▲, Ti_L; △, Ti_L*. Asterisks indicate the relevant statistically significant differences ($p < 0.05$).

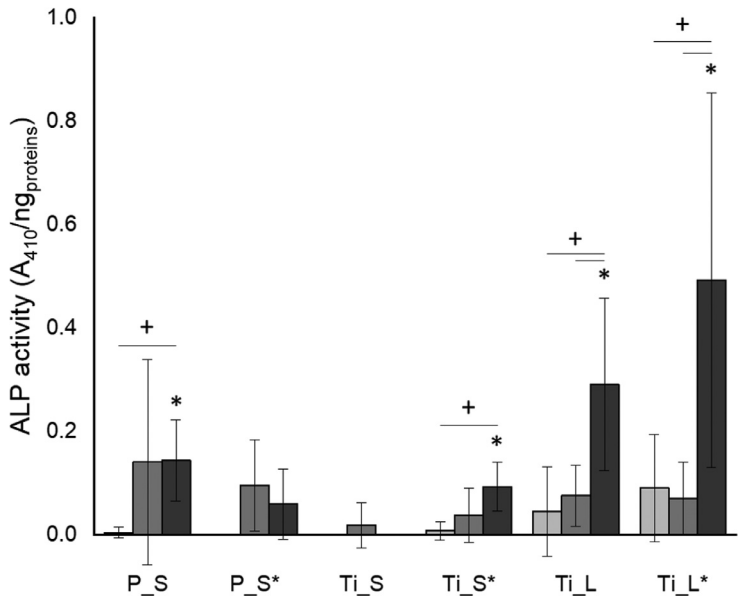

Fig. 7. ALP activity for hDPSCs cultured on treated samples. ALP activity expressed as the absorbance at 410 nm normalized for the amount of proteins measured in each sample at day 4 (light grey), day 7 (grey) and day 14 (dark grey). +, statistically significant differences within sample groups; *, statistically significant differences between groups at the same time point.

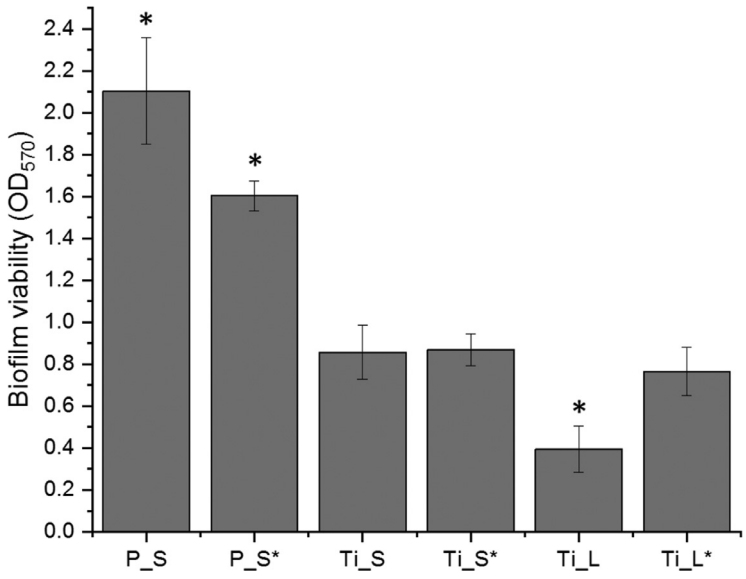

Fig. 8. Biofilm formation on treated samples. Biofilm viability evaluated with the MTT assay. Asterisks indicate the relevant statistically significant differences ($p < 0.05$).

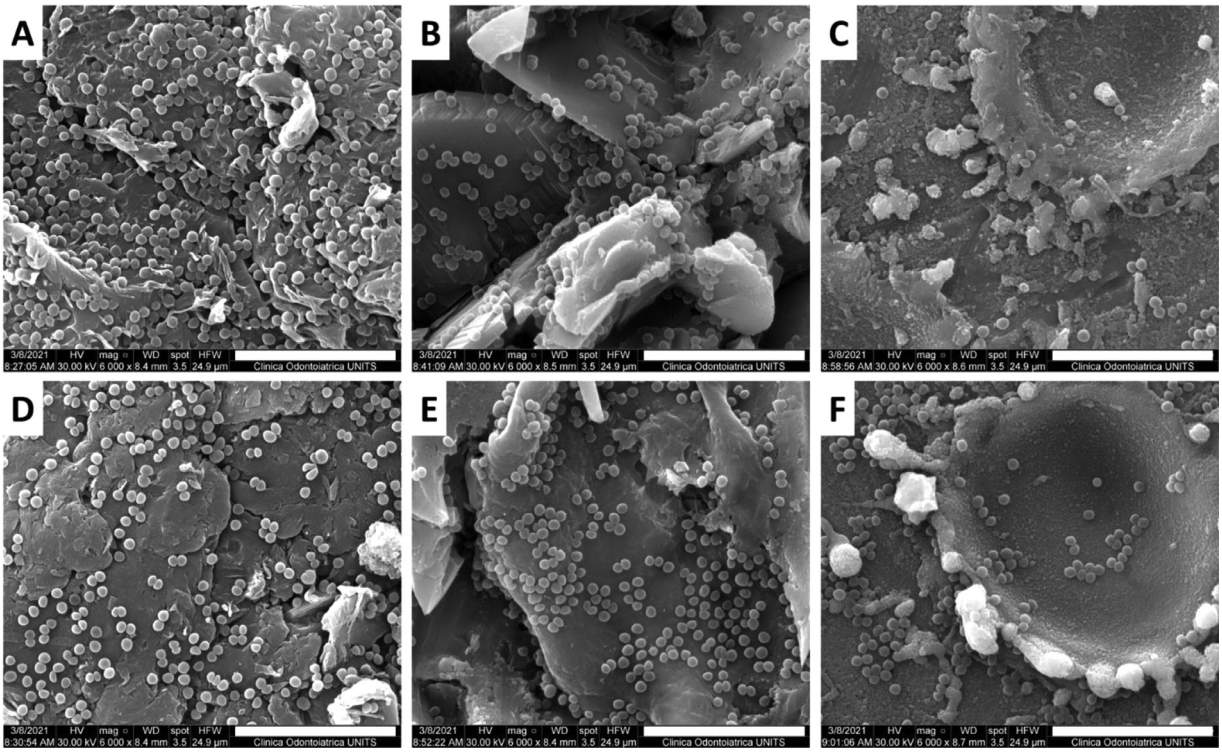

Fig. 9. Bacterial adhesion. SEM micrographs of bacterial cells adhered on samples surfaces: P_S (A), P_S* (D), Ti_S (B), Ti_S* (E), Ti_L (C), Ti_L* (F). Scale bar is 10 µm.

als tested are able to sustain osteoblast adhesion and proliferation, with the best behavior displayed by sandblasted titanium samples.

The behavior of hDPSCs cultured on the tested materials, showed differences with respect to the osteoblasts (MG63). The adhesion was similar on all the materials tested without any statistically significant differences. hDPSCs proliferation was similar on all the tested materials up to 6 days, then an apparent slowdown of proliferation was observed on laser micropatterned titanium surfaces, accompanied by a marked increase of ALP activity with respect to the other materials and treatments. The ALP activity was chosen as a marker of osteoblast differentiation as it has been already used, as an osteo-specific marker, to evaluate the behavior of hDPSCs in seeded in scaffolds or cultured in differentiation conditions [88–92]. Comparing these data with the SEM micrographs of hDPSCs cultured on the tested materials, it can be noted how the differences of the sample chemical nature, wettability and roughness, did not influence hDPSCs proliferation, while affecting cell differentiation towards an osteoblast phenotype. As reported by Berardi *et al.* for SaOS-2 cell line, the ALP activity is higher on laser micropatterned surfaces than on sandblasted surfaces [93]. The behavior of DPSCs seeded on PEEK or titanium is poorly treated in literature, and few works compare titanium to PEEK in terms of osteoblast differentiation. Moreover, there is not a consensus on the behavior of DPSCs on titanium surfaces: while Iaculli *et al.* and Nakamura *et al.* reported a higher mineralized tissue formation on rough titanium samples [4,6], Sushmita *et al.* re-

ported a higher cell growth and extracellular matrix deposition on smoother surfaces [94]. The scientific literature reports the ability of surface modified PEEK to sustain the proliferation and differentiation of DPSCs [95], bone marrow stem cells [31,96] and human fetal osteoblasts [78]. On the contrary, no differences were observed in terms of ALP activity when osteoblasts are seeded on PEEK, titanium or zirconia samples [78].

The effects of the material nature and of the surface morphology and wettability, on bacterial adhesion and biofilm formation, were assessed using *Staphylococcus aureus*, one of the bacterial strains mostly associated with peri-implant infections [10,13,17,97], using the MTT test [98]. Unlike eukaryotic cells behavior, the biofilm formation showed a strong dependence on the materials and on the wettability and roughness. The highest biofilm formation was observed on PEEK samples, and particularly on samples not treated with air plasma cleaning process. Hydrophobic surface chemistry has been associated with bacterial adhesion [10] and it has been demonstrated that sandblasted PEEK is a good substrate for bacterial adhesion. In this context Rochford *et al.* proposed an oxygen plasma treatment for the increase of PEEK surface hydrophilicity, to discourage bacterial adhesion, but failed to obtain a significant effect [10]. In contrast, in the work here presented it was demonstrated that the increase of hydrophilicity led to a decrease of *S. aureus* biofilm formation. Biofilm formation observed on P_S* samples was still higher than the biofilm formation observed on sandblasted titanium samples, indicating that other material characteristics, besides roughness and wettability, affect the bacterial behavior. The lowest biofilm formation was observed, as expected, on laser-treated titanium samples [16,17] not subjected to the air-plasma treatment. This treatment, increasing surface wettability, can enhance bacterial adhesion on this micropatterned surface. Several strategies have been described in the literature for the generation of an antibacterial surface on titanium implants, e.g. coatings with antibiotics, antimicrobial peptides or cationic polymers or the implantation of antibacterial ions [13]. The most used strategies for PEEK are instead the coating with silver nanoparticles [42], silver ions [43], antibiotics [41,99] or antimicrobial polymers [100]. Among these strategies the laser micropatterning proposed by Ionescu *et al.* and Drago *et al.* [16,17] emerges as an interesting strategy which does not requires complex steps of processing or the employment of toxic or hazardous compounds. This process is able preserve the smoothness and the poor wettability of titanium surfaces, which discourage biofilm formation, providing, at the same time a regular pattern recognized by eukaryotic cells as a suitable substrate for the adhesion and growth.

Overall, in the context of this work, the material nature and the surface morphology emerge as important parameters in the interaction with eukaryotic and bacterial cells. The rough surfaces obtained with sandblasting were indeed more prone to induce cell adhesion and proliferation than the smooth surface of laser-treated micropatterned titanium samples, which in contrast, were the most favorable surfaces to sustain hDPSCs differentiation, and the best choice in terms of discouraging of biofilm formation. As the literature reports controversial results in terms of *in vivo* performances of implants and prostheses based on titanium or PEEK, further studies are necessary to determine the best performing material and the best choice of surface treatment in term of osteointegration, osteoinduction and bacterial adhesion. In this context, given the excellent results obtained with titanium micropatterned surfaces, laser micropatterning treatments of PEEK [28,40], developed to improve resin filling, adhesive bonding and shear bond strength, could be an interesting strategy for the improvement of bioactive and antimicrobial properties of PEEK.

The biological analyses performed in this study have been limited to the evaluation of hDPSCs differentiation by the analysis of Alkaline Phosphatase, and the analysis of only one bacterial strain, the *S. aureus*. As the ALP activity is an early marker of osteoblast differentiation, other analyses, such as the quantification of Osteocalcin and Osteopontin, and the analysis of extracellular matrix deposition with Alizarin Red staining, will be useful to investigate more in details the hDPSCs behavior on the tested materials. Regarding the microbiological analyses, Gram negative bacterial strains, such as *Escherichia coli*, and other pathogens involved in the oral cavity and in peri-implantitis formation, such as *Streptococcus mutans*, need to be taken into account to accurately investigate the effects of surface treatments and of biomaterials nature on the efficacy and success of dental implants.

5. Conclusions

Sandblasting and air-plasma treatments were efficient for the increase of surface roughness and wettability of titanium and PEEK samples. The comparison of sandblasted surfaces, with titanium micropatterned surfaces, showed that in this context, the wettability is not the critical parameter for cell adhesion and proliferation, and that the surface topography plays the major role. All the materials tested showed to be able to sustain cell adhesion and proliferation, which was higher on sandblasted samples. Laser-treated micro-patterned titanium proved to be the best choice in terms of discouraging of *S. aureus* biofilm formation, eukaryotic cell proliferation and dental pulp stem cells differentiation; while sandblasted PEEK samples were the less able to prevent biofilm formation. Further analyses are necessary to investigate more in details the osteoblast phenotype of differentiated hDPSCs, to confirm the ability of laser micropatterned titanium to discourage bacterial adhesion and biofilm formation using Gram negative bacteria and other bacterial strains involved in peri-implantitis.

Declaration of Competing Interest

The authors declare that they have no known competing financial interests or personal relationships that could have appeared to influence the work reported in this paper.

Acknowledgments

The authors are grateful to Geass S.r.l. (Italy) for providing titanium samples. The authors are also grateful to Momic's dental technician laboratory (Trieste, Italy), for their help with sandblasting process, and to Dr. Denis Scaini (International School for Advanced Studies, SISSA, Trieste) for his help with the air-plasma treatment.

References

[1] T. El Awadly, G. Wu, M. Ayad, I.A.W. Radi, D. Wismeijer, H.A. El Fetouh, R.B. Osman, Clin. Oral Implants Res. 31 (2020) 246–254.
[2] P. Trisi, M. Berardini, M. Colagiovanni, D. Berardi, G. Perfetti, Implant Dent. 25 (2016) 575–580.
[3] G. Cervino, L. Fiorillo, G. Iannello, D. Santonocito, G. Risitano, M. Cicciù, Materials 12 (2019) 1763.
[4] F. Iaculli, E.S.D. Filippo, A. Piattelli, R. Mancinelli, S. Fulle, J. Biomed. Mater. Res. B Appl. Biomater. 105 (2017) 953–965.
[5] R. Olivares-Navarrete, S.L. Hyzy, R.A. Gittens, J.M. Schneider, D.A. Haithcock, P.F. Ullrich, P.J. Slosar, Z. Schwartz, B.D. Boyan, Spine J. 13 (2013) 1563–1570.
[6] H. Nakamura, L. Saruwatari, H. Aita, K. Takeuchi, T. Ogawa, J. Dent. Res. 84 (2016) 515–520.
[7] L. Canullo, M. Menini, G. Santori, M. Rakic, A. Sculean, P. Pesce, Clin. Oral Investig. 24 (2020) 1113–1124.
[8] L.-C. Zhang, L.-Y. Chen, L. Wang, Adv. Eng. Mater. 22 (2020) 1901258.

[9] N. Iwata, K. Nozaki, N. Horiuchi, K. Yamashita, Y. Tsutsumi, H. Miura, A. Nagai, J. Biomed. Mater. Res. A 105 (2017) 2589–2596.
[10] E.T.J. Rochford, A.H.C. Poulsson, J. Salavarrieta Varela, P. Lezuo, R.G. Richards, T.F. Moriarty, Colloids Surf. B Biointerfaces 113 (2014) 213–222.
[11] K.A. Whitehead, J. Colligon, J. Verran, Colloids Surf. B Biointerfaces 41 (2005) 129–138.
[12] A. Trampuz, W. Zimmerli, Injury 37 (2006) S59–S66.
[13] H. Chouirfa, H. Bouloussa, V. Migonney, C. Falentin-Daudré, Acta Biomater 83 (2019) 37–54.
[14] P. Melicherčík, O. Nešuta, V. Čeřovský, Pharmaceuticals 11 (2018) 20.
[15] J. Chen, F. Wang, Q. Liu, J. Du, Chem. Commun. 50 (2014) 14482–14493.
[16] A.C. Ionescu, E. Brambilla, F. Azzola, M. Ottobelli, G. Pellegrini, L.A. Francetti, PLOS ONE 13 (2018) e0202262.
[17] L. Drago, M. Bortolin, E.D. Vecchi, S. Agrappi, R.L. Weinstein, R. Mattina, L. Francetti, J. Chemother. 28 (2016) 383–389.
[18] R.D. Carpenter, B.S. Klosterhoff, F.B. Torstrick, K.T. Foley, J.K. Burkus, C.S.D. Lee, K. Gall, R.E. Guldberg, D.L. Safranski, J. Mech. Behav. Biomed. Mater. 80 (2018) 68–76.
[19] K.B. Sagomonyants, M.L. Jarman-Smith, J.N. Devine, M.S. Aronow, G.A. Gronowicz, Biomaterials 29 (2008) 1563–1572.
[20] J. Khoury, M. Maxwell, R.E. Cherian, J. Bachand, A.C. Kurz, M. Walsh, M. Assad, R.C. Svrluga, J. Biomed. Mater. Res. B Appl. Biomater. 105 (2017) 531–543.
[21] E.-S.A. Hegazy, T. Sasuga, M. Nishii, T. Seguchi, Polymer 33 (1992) 2904–2910.
[22] M. Savaris, G.A. Carvalho, A. Falavigna, V. dos Santos, R.N. Brandalise, M. Savaris, G.A. Carvalho, A. Falavigna, V. dos Santos, R.N. Brandalise, Mater. Res. 19 (2016) 807–811.
[23] A. Godara, D. Raabe, S. Green, Acta Biomater 3 (2007) 209–220.
[24] X. Han, N. Sharma, Z. Xu, L. Scheideler, J. Geis-Gerstorfer, F. Rupp, F.M. Thieringer, S. Spintzyk, J. Clin. Med. 8 (2019) 771.
[25] X. Han, D. Yang, C. Yang, S. Spintzyk, L. Scheideler, P. Li, D. Li, J. Geis-Gerstorfer, F. Rupp, J. Clin. Med. 8 (2019) 240.
[26] P. Honigmann, N. Sharma, B. Okolo, U. Popp, B. Msallem, F.M. Thieringer, BioMed Res. Int. 2018 (2018) 4520636.
[27] J. Ma, Q. Liang, W. Qin, P.O. Lartey, Y. Li, X. Feng, J. Mech. Behav. Biomed. Mater. 102 (2020) 103497.
[28] B. Henriques, D. Fabris, J. Mesquita-Guimarães, A.C. Sousa, N. Hammes, J.C.M. Souza, F.S. Silva, M.C. Fredel, J. Mech. Behav. Biomed. Mater. 84 (2018) 225–234.
[29] T. Elawadly, I.A.W. Radi, A. El Khadem, R.B. Osman, J. Oral Implantol. 43 (2017) 456–461.
[30] S. Verma, N. Sharma, S. Kango, S. Sharma, Eur. Polym. J. 147 (2021) 110295.
[31] S. Mishra, R. Chowdhary, Clin. Implant Dent. Relat. Res. 21 (2019) 208–222.
[32] D. Williams, Med. Device Technol. 12 (2001) 8–9.
[33] J. Wu, L. Shi, Y. Pei, D. Yang, P. Gao, X. Xiao, S. Guo, M. Li, X. Li, Z. Guo, Eur. Spine J. 29 (2020) 1159–1166.
[34] F.B. Torstrick, A.S.P. Lin, D.L. Safranski, D. Potter, T. Sulchek, C.S.D. Lee, K. Gall, R.E. Guldberg, Spine 45 (2020) E417.
[35] M. Junaid, M.U. Rashid, S.S. Bukhari, M. Ahmed, Pak. J. Med. Sci. 34 (2018) 1412–1417.
[36] M. Mounir, M. Shalash, S. Mounir, Y. Nassar, O.E. Khatib, Clin. Implant Dent. Relat. Res. 21 (2019) 960–967.
[37] B. Schliemann, R. Seifert, C. Theisen, D. Gehweiler, D. Wähnert, M. Schulze, M.J. Raschke, A. Weimann, Arch. Orthop. Trauma Surg. 137 (2017) 63–71.
[38] S. Najeeb, Z.K. Bds, S.Z. Bds, M.S.Z. Bds, J. Oral Implantol. 42 (2016) 512–516.
[39] A.Tsuchiya Sunarso, N. Fukuda, R. Toita, K. Tsuru, K. Ishikawa, J. Biomater. Sci. Polym. Ed. 29 (2018) 1375–1388.
[40] C.K. Akkan, M. Hammadeh, S. Brück, H.W. Park, M. Veith, H. Abdul-Khaliq, C. Aktas, Mater. Lett. 109 (2013) 261–264.
[41] N.C. Lau, M.H. Tsai, D.W. Chen, C.H. Chen, K.W. Cheng, Appl. Sci. 10 (2020) 97.
[42] L. Deng, Y. Deng, K. Xie, Colloids Surf. B Biointerfaces 160 (2017) 483–492.
[43] X. Liu, K. Gan, H. Liu, X. Song, T. Chen, C. Liu, Dent. Mater. 33 (2017) e348–e360.
[44] A. Xu, L. Zhou, Y. Deng, X. Chen, X. Xiong, F. Deng, S. Wei, J. Mater. Chem. B 4 (2016) 1878–1890.
[45] D. Gravis, F. Poncin-Epaillard, J.-F. Coulon, Plasma Process. Polym. 15 (2018) 1800007.
[46] S. Bosi, R. Rauti, J. Laishram, A. Turco, D. Lonardoni, T. Nieus, M. Prato, D. Scaini, L. Ballerini, Sci. Rep. 5 (2015) 9562.
[47] A.E. Wiącek, K. Terpiłowski, M. Jurak, M. Worzakowska, Polym. Test. 50 (2016) 325–334.
[48] I.-H. Kim, J.S. Son, T.-Y. Kwon, K.-H. Kim, J. Nanosci. Nanotechnol. 15 (2015) 134–137.
[49] D. Rymuszka, K. Terpiłowski, P. Borowski, L. Holysz, Polym. Int. 65 (2016) 827–834.
[50] E. Ledesma-Martínez, V.M. Mendoza-Núñez, E. Santiago-Osorio, Stem Cells Int 2015 (2015) 4709572.
[51] P.D. Potdar, Y.D. Jethmalani, World J. Stem Cells 7 (2015) 839–851.
[52] R. Núñez-Toldrà, E. Martínez-Sarrà, C. Gil-Recio, M.Á. Carrasco, A. Al Madhoun, S. Montori, M. Atari, BMC Cell Biol. 18 (2017) 21.
[53] C. Palumbo, A. Baldini, F. Cavani, P. Sena, M. Benincasa, M. Ferretti, D. Zaffe, Micron 47 (2013) 1–9.
[54] M.G. McCormack, A.J. Smith, A.N. Akram, M. Jackson, D. Robertson, G. Edwards, Am. J. Infect. Control 43 (2015) 35–37.
[55] M. Giannelli, G. Landini, F. Materassi, F. Chellini, A. Antonelli, A. Tani, S. Zecchi-Orlandini, G.M. Rossolini, D. Bani, Lasers Med. Sci. 31 (2016) 1613–1619.
[56] T. Thurnheer, G.N. Belibasakis, Clin. Oral Implants Res. 27 (2016) 890–895.
[57] B. Sinjari, T. Traini, S. Caputi, C. Mortellaro, A. Scarano, J. Craniofac. Surg. 29 (2018) 2277–2281.
[58] H. Wang, D.T.K. Kwok, M. Xu, H. Shi, Z. Wu, W. Zhang, P.K. Chu, Adv. Mater. 24 (2012) 3315–3324.
[59] M.J. Shenton, G.C. Stevens, N.P. Wright, X. Duan, J. Polym. Sci. Part Polym. Chem. 40 (2002) 95–109.
[60] E.M. Liston, L. Martinu, M.R. Wertheimer, J. Adhes. Sci. Technol. 7 (1993) 1091–1127.
[61] S. Giljean, M. Bigerelle, K. Anselme, Scanning 36 (2014) 2–10.
[62] H. Deng, S. Molins, D. Trebotich, C. Steefel, D. DePaolo, Geochim. Cosmochim. Acta 239 (2018) 374–389.
[63] T. Bodner, A. Behrendt, E. Prax, F. Wiesbrock, Monatshefte Für Chem. - Chem. Mon. 143 (2012) 717–722.
[64] A.D. Schwitalla, F. Bötel, T. Zimmermann, M. Sütel, W.-D. Müller, Dent. Mater. 33 (2017) 990–994.
[65] R. Ourahmoune, M. Salvia, T.G. Mathia, N. Mesrati, Scanning 36 (2014) 64–75.
[66] D. Quéré, Annu. Rev. Mater. Res. 38 (2008) 71–99.
[67] T.S. Vira, S.K. Zaaba, M.T. Mustaffa, J. Phys. Conf. Ser. 1372 (2019) 012010.
[68] A. Xu, X. Liu, X. Gao, F. Deng, Y. Deng, S. Wei, Mater. Sci. Eng. C 48 (2015) 592–598.
[69] S.S. da Rocha, G.L. Adabo, G.E.P. Henriques, M.A. de A. Nóbilo, Braz. Dent. J. 17 (2006) 126–129.
[70] R.K. Goyal, A.N. Tiwari, Y.S. Negi, Mater. Sci. Eng. A 491 (2008) 230–236.
[71] E. Denes, G. Barriere, E. Poli, G. Leveque, J. Long. Term Eff. Med. Implants 28 (2018) 9–13.
[72] M. Rahmati, M. Mozafari, J. Cell. Physiol. 234 (2019) 3321–3335.
[73] A. Piattelli, M. Degidi, M. Paolantonio, C. Mangano, A. Scarano, Biomaterials 24 (2003) 4081–4089.
[74] S.A. Gehrke, S. Taschieri, M. Del Fabbro, P.G. Coelho, J. Oral Implantol. 41 (2015) 515–522.
[75] H. Kim, S.-H. Choi, J.-J. Ryu, S.-Y. Koh, J.-H. Park, I.-S. Lee, Biomed. Mater. 3 (2008) 025011.
[76] L. Saldaña, V. Barranco, J.L. González-Carrasco, M. Rodríguez, L. Munuera, N. Vilaboa, J. Biomed. Mater. Res. A 81A (2007) 334–346.
[77] M. Gheisarifar, G.A. Thompson, C. Drago, F. Tabatabaei, M. Rasoulianboroujeni, J. Prosthet. Dent. (2020).
[78] M.B. da Cruz, J.F. Marques, G.M. Penarrieta-Juanito, M. Costa, J.C.M. Souza, R.S. Magini, G. Miranda, F.S. Silva, A.D.S.P. da Mata, J.M.M. Carames, Int. J. Oral Maxillofac. Implants 34 (2019) 1–27.
[79] F.B. Torstrick, A.S.P. Lin, D. Potter, D.L. Safranski, T.A. Sulchek, K. Gall, R.E. Guldberg, Biomaterials 185 (2018) 106–116.
[80] J. O'Brien, I. Wilson, T. Orton, F. Pognan, Eur. J. Biochem. 267 (2000) 5421–5426.
[81] S.L. Voytik-Harbin, A.O. Brightman, B. Waisner, C.H. Lamar, S.F. Badylak, Vitro Cell. Dev. Biol. - Anim. 34 (1998) 239–246.
[82] P. Sacco, G. Baj, F. Asaro, E. Marsich, I. Donati, Adv. Funct. Mater. 30 (2020) 2001977.
[83] K. Benz, A. Schöbel, M. Dietz, P. Maurer, J. Jackowski, Materials 12 (2019) 2739.
[84] L.L. Ramenzoni, T. Attin, P.R. Schmidlin, Materials 12 (2019) 1401.
[85] J. Guillem-Marti, L. Delgado, M. Godoy-Gallardo, M. Pegueroles, M. Herrero, F.J. Gil, Clin. Oral Implants Res. 24 (2013) 770–780.
[86] C.J. Oates, W. Wen, D.W. Hamilton, Materials 4 (2011) 893–907.
[87] J.I. Rosales-Leal, M.A. Rodríguez-Valverde, G. Mazzaglia, P.J. Ramón-Torregrosa, L. Díaz-Rodríguez, O. García-Martínez, M. Vallecillo-Capilla, C. Ruiz, M.A. Cabrerizo-Vílchez, Colloids Surf. Physicochem. Eng. Asp. 365 (2010) 222–229.
[88] M. Alipour, N. Firouzi, Z. Aghazadeh, M. Samiei, S. Montazersaheb, A.B. Khoshfetrat, M. Aghazadeh, BMC Biotechnol 21 (2021) 6.
[89] L.M. Escobar, J.D. Escobar, Z. Bendahan, J.E. Castellanos, J. Oral Biol. Craniofacial Res. 11 (2021) 143–148.
[90] R. Moonesi Rad, D. Atila, E.E. Akgün, Z. Evis, D. Keskin, A. Tezcaner, Mater. Sci. Eng. C 100 (2019) 928–948.
[91] T. Okajcekova, J. Strnadel, M. Pokusa, R. Zahumenska, M. Janickova, E. Halasova, H. Skovierova, Int. J. Mol. Sci. 21 (2020) 2280.
[92] N.K. Oliveira, T.H.C. Salles, A.C. Pedroni, L. Miguita, M.A. D'Ávila, M.M. Marques, M.C.Z. Deboni, Dent. Mater. 35 (2019) 1740–1749.
[93] D. Berardi, S. De Benedittis, A. Polimeni, C. Malagola, C. Cassinelli, G. Perfetti, Int. J. Immunopathol. Pharmacol. 22 (2009) 125–131.
[94] V.P. Sushmita, J.S.C. Kumar, C. Hegde, B.G.S. Kurkalli, J. Osseointegration 11 (2019) 553–560.
[95] J. Khoury, I. Selezneva, S. Pestov, V. Tarassov, A. Ermakov, A. Mikheev, M. Lazov, S.R. Kirkpatrick, D. Shashkov, A. Smolkov, Bioact. Mater. 4 (2019) 132–141.
[96] Y. Zhao, H.M. Wong, W. Wang, P. Li, Z. Xu, E.Y.W. Chong, C.H. Yan, K.W.K. Yeung, P.K. Chu, Biomaterials 34 (2013) 9264–9277.
[97] J. Parvizi, K. Azzam, E. Ghanem, M.S. Austin, R.H. Rothman, Clin. Orthop. Relat. Res. 467 (2009) 1732–1739.
[98] M. Mardirossian, A. Pompilio, V. Crocetta, S. De Nicola, F. Guida, M. Degasperi, R. Gennaro, G. Di Bonaventura, M. Scocchi, Amino Acids 48 (2016) 2253–2260.
[99] X. Xu, Y. Li, L. Wang, Y. Li, J. Pan, X. Fu, Z. Luo, Y. Sui, S. Zhang, L. Wang, Y. Ni, L. Zhang, S. Wei, Biomaterials 212 (2019) 98–114.
[100] M.H. Abdulkareem, A.H. Abdalsalam, A.J. Bohan, Prog. Org. Coat. 130 (2019) 251–259.